

Overexpression and properties of a new thermophilic and thermostable esterase from *Bacillus acidocaldarius* with sequence similarity to hormone-sensitive lipase subfamily

Giuseppe MANCO*, Elena ADINOLFI*, Francesca M. PISANI*, Gianluca OTTOLINA†, Giacomo CARREA† and Mosè ROSSI*‡¹

*Istituto di Biochimica delle Proteine ed Enzimologia, CNR, Via Marconi 10, 80125 Naples, Italy, †Istituto di Chimica degli Ormoni, CNR, Via Mario Bianco 9, 20131, Milano, Italy, and ‡Università degli Studi di Napoli Federico II, Via Mezzocannone 16, 80100, Naples, Italy

We previously purified a new esterase from the thermoacidophilic eubacterium *Bacillus acidocaldarius* whose N-terminal sequence corresponds to an open reading frame (ORF3) reported to show homology with the mammalian hormone-sensitive lipase (HSL)-like group of the esterase/lipase family. To compare the biochemical properties of this thermophilic enzyme with those of the homologous mesophilic and psychrophilic members of the HSL group, an overexpression system in *Escherichia coli* was established. The protein, expressed in soluble and active form at 10 mg/l *E. coli* culture, was purified to homogeneity and characterized biochemically. The enzyme, a 34 kDa monomeric protein, was demonstrated to be a B'-type carboxylesterase (EC 3.1.1.1) on the basis of substrate specificity and the action of inhibitors. Among the *p*-nitrophenyl (PNP) esters tested the best substrate was PNP-exanoate with K_m and k_{cat} values of $11 \pm 2 \mu\text{M}$ (mean \pm S.D., $n = 3$) and $6610 \pm 880 \text{ s}^{-1}$ (mean \pm S.D., $n = 3$)

respectively at 70 °C and pH 7.1. In spite of relatively high sequence identity with the mammalian HSLs, the psychrophilic *Moraxella* TA144 lipase 2 and the human liver arylacetamide deacetylase, no lipase or amidase activity was detected. A series of substrates were tested for enantioselectivity. Substantial enantioselectivity was observed only in the resolution of (\pm)-3-bromo-5-(hydroxymethyl)- Δ^2 -isoxazoline, where the (*R*)-product was obtained with an 84% enantiomeric excess at 36% conversion. The enzyme was also able to synthesize acetyl esters when tested in vinyl acetate and toluene. Inactivation by diethylpyrocarbonate, diethyl-*p*-nitrophenyl phosphate, di-isopropylphosphofluoridate (DFP) and physostigmine, as well as labelling with [³H]DFP, supported our previous suggestion of a catalytic triad made up of Ser-His-Asp. The activity–stability–temperature relationship is discussed in relation to those of the homologous members of the HSL group.

INTRODUCTION

Studies [1,2] have suggested that esterases, lipases and cholinesterases belong to a large family of phylogenetically related proteins, which includes representatives in the domains of Eukarya and Bacteria and proteins lacking enzymic activity. Three subfamilies have been identified: the C group includes cholinesterases from vertebrates and invertebrates, lipases from fungi, a number of esterases and some non-enzymic proteins; group L includes lipases from vertebrates and bacteria, lipoprotein lipases, lecithin:cholesterol acyltransferases and related non-enzymic vitellogenins from flies; the third group was named hormone-sensitive lipase (HSL) by Hemilä et al. [1], because these authors reported the cloning and sequencing of a gene from *Bacillus acidocaldarius* encoding a protein of unknown function [open reading frame (ORF3)], sharing homology with the HSL from human and rat [3]. In this group were included also the *N*-acetylphosphino-thricin tripeptide deacetylase from *Streptomyces hygroscopicus* [4], the acetylhydrolase from *Streptomyces viridochromogenes* [5], the lipase 2 from *Moraxella* TA144 (MOL) [6], an esterase from *Acinetobacter calcoaceticus* (ACE) [7] and from *Escherichia coli* [8], Vsh5, a protein from the slime mould *Dictyostelium discoideum* [9], and the recently sequenced human liver arylacetamide deacetylase (HDAC) [10]. Unfortunately,

it is unclear at present whether this sequence similarity implies comparable biochemical properties for these enzymes.

Lipases are scarcely active against soluble esters or insoluble esters in a monodisperse form. However, they become markedly activated when the substrate solubility (or critical micellar concentration) is exceeded, a phenomenon called interfacial activation. In contrast, simple esterases or carboxylesterases do not obey this rule, a finding described quantitatively for the first time in 1958 by Sarda and Deusnelle [11]. Despite this simple distinction, results have been accumulated in the last few years that challenge this classical concept. Cutinases, for example, although able to hydrolyse the classical lipases substrates, do not show the interfacial activation phenomenon [12], representing a bridge between lipases and esterases. New enzymes from thermophilic bacteria could add new insights into the evolutionary relationships in the esterase/lipase family on the one hand; on the other hand they could allow fundamental studies in the field of protein stability for this class of proteins. Moreover they are giving rise to growing interest in the biotransformations field.

So far, carboxylesterases have been purified and partially characterized only from *Sulfolobus acidocaldarius* [13], *Bacillus stearothermophilus* [14–16] and *Bacillus acidocaldarius* [17]. A lipase has been isolated from *Bacillus thermocatenuatus* [18].

Abbreviations used: ACE, *Acinetobacter calcoaceticus* esterase; DFP, di-isopropylphosphofluoridate; EST2, esterase 2; HDAC, human arylacetamide deacetylase; HSL, hormone-sensitive lipase; IPTG, isopropyl β -D-thiogalactoside; MOL, *Moraxella* TA144 lipase 2; ORF, open reading frame; PNP, *p*-nitrophenyl.

¹ To whom correspondence should be addressed at the Istituto di Biochimica delle Proteine ed Enzimologia (e-mail manco@dafne.ibpe.na.cnr.it).

We recently reported the purification of a new esterase from *B. acidocaldarius* and demonstrated its identity with the aforementioned ORF3 [19].

Here we describe the overexpression in *E. coli* of this gene, kindly provided by Professor I. Palva [20], the purification of the recombinant protein and some biochemical studies done to obtain further insight into the structure–function relationship of this interesting representative of the HSL group.

EXPERIMENTAL

Materials

p-Nitrophenyl (PNP) esters, PNP-acetamide, Fast Blue RR and β -naphthylacetate, were purchased from Sigma Chemical Co. (St. Louis, MO, U.S.A.). Molecular mass markers for SDS/PAGE and for gel-filtration chromatography were obtained from Pharmacia LKB. [³H]Di-isopropylphosphofluoridate (DFP) (6 Ci/mmol) and [¹⁴C]trioleoylglycerol (60 Ci/mol) were from Amersham.

Strains and plasmids

E. coli Top 10 (Invitrogen) was used as host for cloning; *E. coli* BL21(DE3) harboured the recombinant plasmid for gene expression. The expression vectors utilized were two derivatives (pT7-7 and pT7-SCII) of vector pT7 [21,22].

Cloning and overexpression

Standard molecular cloning techniques were employed [23]. *E. coli* cells [Top 10 or BL21(DE3)] were grown at 37 °C in Luria–Bertani medium containing ampicillin at 100 μ g/ml. Modification and restriction enzymes used in this work were from Promega and were used under the conditions recommended by the supplier.

A 1540 bp fragment containing the entire ORF3 with its promoter and RBS sequences was released from plasmid pKTH2000 [20], a pBR322 derivative. It was ligated into the unique *Pst*I site of expression vector pT7-SCII. This construct, referred to as pT7-SCII-GM1, was transformed into BL21(DE3) cells and induction was started when the culture reached a D_{600} of 1.8 units, by adding isopropyl β -D-thiogalactoside (IPTG) to a final concentration of 0.5 mM and continuing the incubation at 37 °C for an additional 3 h. For large-scale protein production, 10 litres of Luria–Bertani medium containing 100 μ g/ml ampicillin were inoculated at a D_{600} of 0.005 and grown overnight at 37 °C with vigorous bubbling of sterile air. The next day, after 3 h of IPTG induction, cells were harvested by centrifugation (3000 g, 4 °C, 15 min), washed with 25 mM Tris/HCl buffer (pH 8.4)/2.5 mM MgCl₂/0.5 mM EDTA/1 mM dithiothreitol (buffer A) and stored at –70 °C.

Purification of the recombinant enzyme

All procedures were performed at room temperature unless indicated otherwise. Wet frozen cells (40 g) were thawed and resuspended in 150 ml of buffer A. Aliquots of 40 ml were broken by passing through a French pressure cell apparatus (Aminco Co., Silver Spring, MD, U.S.A.). A pressure setting of 2000 lb/in² (1.38 MPa) was used. Cell debris was removed by centrifugation (80000 g, 30 min, 4 °C). The crude extract after dilution 1:1 with buffer A was thermoprecipitated as follows: 5 min incubation at 60, 65 then 70 °C, under gentle stirring and with clarification by centrifugation (17000 g, 30 min, 4 °C) between steps. Pellets were discarded. The final enzyme solution was directly loaded on a column (20 cm \times 3 cm) of Q Sepharose

Fast Flow (Pharmacia) equilibrated with buffer A, at 4 °C. The flow rate was 30 ml/h. After the column had been washed, a linear gradient (150 ml plus 150 ml) of increasing NaCl concentration (from 0 to 1 M) was applied. The active fractions from the previous step were pooled, brought to 10% (w/v) (NH₄)₂SO₄ and applied directly to an FPLC phenyl-Superose column (10 cm \times 3 cm; Pharmacia) equilibrated in buffer A, containing 10% -satd. (NH₄)₂SO₄. After the column had been washed, a decreasing gradient of (NH₄)₂SO₄ [10% to 0% (w/v)] was applied. Activity was split into two peaks (a and b) of different specific activities. The enzyme from peak (a) was pure after this step; active fractions were pooled, concentrated by ultrafiltration to 2–3 mg/ml and stored at 4 °C. The enzyme from peak (b) was not pure after this step; active fractions were pooled and loaded on an FPLC Mono Q Sepharose Fast Flow column (10 cm \times 1 cm; Pharmacia) equilibrated in buffer A. After the column had been washed, elution was performed at a flow rate of 1 ml/min with a linear gradient from 0 to 500 mM NaCl in buffer A. The most active fractions were pooled, concentrated and stored at 4 °C. These two enzymes preparations were indistinguishable by molecular mass in native or denaturing conditions, but enzyme from peak (b) displayed a lower specific activity that could be due to a post-translational modification and/or to a folding problem. Only enzyme from peak (a) was used for further experiments. It was stored at 4 °C or at –20 °C [after the addition of 50% (v/v) glycerol] and was stable for at least 6 and 12 months respectively.

Enzyme assays

The time course of the esterase-catalysed hydrolysis of PNP esters was followed by monitoring the production of *p*-nitrophenoxide at 405 nm in 1 cm pathlength cells with a double-beam Varian Cary1E UV–visible spectrophotometer equipped with a temperature controller (Varian) based on Peltier heat-exchange devices. Initial rates were calculated by linear least-squares analysis of time courses comprising less than 10% of the total substrate turnover. The standard assay contained 0.2 mM PNP-exanoate in 40 mM Na₂HPO₄/NaH₂PO₄/0.09% (w/v) gum arabic/0.36% (v/v) Triton X-100/2% (v/v) propan-2-ol (pH 7.1) at 70 °C. Stock solutions of PNP esters were prepared by dissolving substrates in water at their maximum of solubility (for kinetic measurements) or in propan-2-ol (for routine assays). The background hydrolysis of the substrate was deducted by using a reference sample of identical composition to the incubation mixture except that esterase was omitted.

One unit of enzymic activity was defined as the amount of protein releasing 1 μ mol of *p*-nitrophenoxide/min from PNP ester at the indicated temperature. The absorption coefficients were measured at each indicated temperature and ranged over 14000–21000 M⁻¹·cm⁻¹. The pH was always adjusted for the appropriate working temperature.

The protein concentration was measured with the Bio-Rad Protein Assay system, with BSA (Fraction V) as standard.

Determination of pH optimum

The dependence of initial velocity on pH was monitored at 348 nm (the pH-independent isosbestic point of *p*-nitrophenol and the *p*-nitrophenoxide ion), with a molar absorption coefficient of 5300 M⁻¹·cm⁻¹, at 70 °C. The buffer used was 0.345 M Tris/HCl over the range 5.6–8.1, or 0.04 M Na₂HPO₄/NaH₂PO₄ over the pH range 6.0–7.5. pH values were adjusted at 70 °C. Data were analysed as described [24].

Kinetic measurements

Initial-velocity–substrate concentration data were fitted to the Lineweaver–Burk transformation of the Michaelis–Menten equation, by weighted linear least-squares analysis with a personal computer and the GRAFIT program [25].

Inhibition studies

The action of several inhibitors was studied. The enzyme (67.5 $\mu\text{g}/\text{ml}$) was incubated at 37 °C in 50 mM Tris/HCl, pH 8, for 5 min with different concentrations of the inhibitor. The reactions were stopped by chilling on ice, and aliquots (2–4 μl) were assayed by the standard assay.

Thermostability and thermophilicity

Enzyme stability was studied over the temperature range 70–90 °C. Pure enzyme (125 $\mu\text{g}/\text{ml}$ in buffer A) was incubated in sealed glass tubes. Aliquots were withdrawn at times and assayed at 70 °C by the standard assay. To calculate $t_{1/2}$ values experimental data points were computer fitted to an equation describing a single exponential decay, with the program GRAFIT [25]. The dependence of enzymic activity on temperature was studied over the range 5–90 °C with PNP-exanoate (90 μM) dissolved in 40 mM phosphate buffer, pH 7.1, without detergents.

Amidase activity was assayed with PNP-acetamide, as described [26]. Lipase activity was assayed with [^{14}C]trioleoyl-glycerol, as described [27].

Electrophoreses

Electrophoretic runs were performed with a Bio-Rad Mini-Protein II cell unit, at room temperature. SDS/PAGE was performed essentially as described by Laemmli [28]. Gels were stained with Coomassie Brilliant Blue G-250 or by silver staining (Sigma). Molecular mass markers (Pharmacia) were phosphorylase *b* (94 kDa), BSA (67 kDa), ovalbumin (43 kDa), carbonic anhydrase (30 kDa), soybean trypsin inhibitor (20.1 kDa) and α -lactalbumin (14.4 kDa). The molecular mass of the denatured enzyme was obtained by interpolation on a plot of the log of molecular mass against relative migrations (R_f values). Non-denaturing PAGE was performed at basic pH (separating gel pH 8.8; running buffer pH 8.3) with 7.5% or 10% (w/v) polyacrylamide slab gels.

Reverse-phase HPLC

Protein purity was also checked by reverse-phase HPLC on a Pharmacia-LKB apparatus. Pure esterase (20 μg) was applied to the column (C_{18} ; Aquapore RP 300; Brownlee) in 200 μl of 0.1% (v/v) trifluoroacetic acid. Elution was performed with a linear gradient from 0.1% trifluoroacetic acid to 70% (v/v) acetonitrile containing 0.1% trifluoroacetic acid. The absorption was monitored at 280 and 220 nm.

Activity staining

Non-denaturing gels and SDS gels after protein renaturation were stained for esterase activity as described [29]. In brief, gels were incubated in a solution (100 ml) of 100 mM Tris/HCl, pH 7.5, containing 5 mg of β -naphthylacetate (dissolved in 0.5 ml of methanol) and 25 mg of Fast Blue RR at room temperature. Reactions were stopped after 15–30 min by rinsing with tap water and placing the gels into 7.5% (v/v) acetic acid.

Molecular mass determination by analytical gel filtration

Pure esterase (100 μg) and protein markers (100 μg) were chromatographed through a Zorbax GF 450 HPLC column (Dupont). The equilibration and elution buffer was 50 mM phosphate, pH 7.2, containing 120 mM NaCl; the flow rate was 1 ml/min. The molecular mass markers used were apoferritin (473 kDa), aldolase (160 kDa), BSA (67 kDa), carbonic anhydrase (29 kDa) and cytochrome *c* (12.6 kDa). Proteins were detected at 280 and 220 nm and esterase activity was measured by the standard assay. The esterase molecular mass was calculated by interpolation on a plot of log molecular mass against the V_e/V_0 ratio.

Active-site serine titration

Pure esterase (2 nmol in 0.5 ml of 20 mM Tris/HCl, pH 8) was titrated by the addition of 23 μl of [^3H]DFP (6 Ci/mmol; 167 pmol/ μl ; 4.6×10^5 c.p.m./ μl) and incubation at 37 °C. Aliquots were withdrawn at intervals from the reaction mixture; the residual activity was assayed by the standard assay. After complete inactivation the enzyme was separated from unreacted [^3H]DFP by gel filtration through a column (20 cm \times 0.5 cm) of Sephadex G-25 equilibrated and eluted with 40 mM phosphate buffer, pH 7. Protein eluted at the void volume was assayed by Bio-Rad protein assay and the co-eluted radioactivity was measured by using a Packard Tri-Carb 300 liquid-scintillation counter.

Enzyme labelling with [^3H]DFP and fluorography

Samples of 5–50 μg of protein were labelled by incubation with 2 μCi of [^3H]DFP in 25 μl of 50 mM phosphate buffer, pH 7, containing 150 mM NaCl, at room temperature for 1 h. After the reaction the unreacted inhibitor was separated from protein by gel filtration through Sephadex G-25. The recovered material was concentrated, the radioactivity was measured by using a Packard Tri-Carb 300 liquid-scintillation counter and aliquots corresponding to 10^3 – 10^4 c.p.m. were subjected to SDS/PAGE. After being run, gels were treated for fluorography as described [30].

Thiol titration

Thiol group titration was performed with Ellman's reagent, as described [31].

N-terminal amino acid sequence analysis

N-terminal amino acid sequence analysis was performed after protein separation by SDS/PAGE and electrotransfer to PVDF membrane (ProBlott; Applied Biosystems), as described by Matsudaira [32]. The band of interest was cut out and subjected to automated Edman degradation with an Applied Biosystems gas-phase sequencer (model 477 A) equipped with an on-line 120 A phenylthiohydantoin analyser, in accordance with the manufacturer's instructions.

CD

Far-UV (190–240 nm) CD measurements were performed in a spectropolarimeter model J-710 (Jasco, Tokyo, Japan) at room temperature under nitrogen flow. A cuvette (Helma, Jamaica, NY, U.S.A.) of 0.1 cm pathlength was used. A spectral

acquisition spacing of 0.2 nm (1.0 nm bandwidth) was used. Each spectrum was averaged ten times and smoothed with Spectropolarimeter System Software Version 1.00 (Jasco).

Antiserum production

Antiserum against esterase 2 (EST2) was developed in rabbits (New Zealand) by subcutaneous injections of 1 mg of purified antigen mixed with an equal volume of Freund's complete adjuvant. The protocol used was: 100 μ g three times and 300 μ g as the last injection at 2-day intervals; then 400 μ g after 28 days from the first injection. At 2 weeks from the last injection rabbits were bled from ear arteries, the antiserum was heated for 30 min at 56 °C to destroy complement, supplemented with 50% (v/v) glycerol and stored at -20 °C.

Western-blot analysis

After the electrophoretic runs, SDS gels were transferred to a nitrocellulose sheet in 0.375 M Tris/glycine buffer, pH 8.3, containing 20% (v/v) methanol, with the Bio-Rad Trans-Blot apparatus. After 1 h at 100 V the nitrocellulose sheet was removed, soaked in 20 mM Tris/HCl buffer, pH 7.5, containing 3% (w/v) BSA (blocking buffer) and incubated for 1 h with the EST2 antiserum diluted 1:1000 in blocking buffer; then the membrane was washed three times for 15 min with 20 mM Tris/HCl buffer, pH 7.5, containing 0.05% (v/v) Tween 20 and 0.5 M LiCl (washing buffer). The filter was incubated for 1 h with goat anti-(rabbit IgG) conjugated with peroxidase (Sigma), diluted 1:2000 in blocking buffer. The filter was washed as described previously and developed by incubation in 0.1 M Tris/HCl buffer, pH 7.6, containing 3,3'-diaminobenzidine (0.3 mg/ml) and H₂O₂ (0.01%).

Enzyme-catalysed resolutions

The following racemic butyrates were subjected to enzymic hydrolysis (see Table 3 for structures): (\pm)-*cis*-2-hydroxymethyl-5-iodomethyltetrahydrofuran (**1**), (\pm)-3-hydroxymethyl-3a,4,5,6,7,7a-hexahydrobenzo[d]isoxazole (**2**), (\pm)-3-hydroxymethyl-3a,5,6,7a-tetrahydro-1,4-dioxino[2,3-d]isoxazole (**3**), (\pm)-3-bromo-5-(hydroxymethyl)- Δ^2 -isoxazoline (**4**) and (\pm)-6-methyl-5-hepten-2-ol (**5**). The following procedure was adopted: the substrate (100 mg) was dissolved in acetonitrile (1 ml) and added to 10 ml of 0.1 M potassium phosphate buffer, pH 7, containing the enzyme (5–50 μ g, depending on the substrate).

The enzyme was stable in the reported conditions for several hours (results not shown). The reaction mixture was stirred at room temperature for a scheduled time (10–30 min, depending on the substrate), extracted three times with 10 ml of ethyl acetate, dried over sodium sulphate and analysed by chiral HPLC or GLC to determine the degree of conversion and the enantiomeric excess of the alcohol products.

With (\pm)-6-methyl-5-hepten-2-ol (**6**) and (\pm)-3-methyl-2-cyclohexen-1-ol (**7**), resolution through transesterification with vinyl acetate in toluene was also performed. The substrate (20 mg) was dissolved in 2 ml of toluene containing 5% (v/v) vinyl acetate and 150 μ g of enzyme (adsorbed on 100 mg of Celite), pre-equilibrated at a water activity value of 0.85 [33]. The reaction mixture was shaken at room temperature for a scheduled time and then analysed for conversion and enantiomeric excess of the products.

Determination of the degree of conversion and enantiomeric excesses

Both the degree of conversion and the enantiomeric excess of the products were determined by chiral GLC for **1**, **2**, **5**, **6** and **7** [33–35] or chiral HPLC for **3** and **4** [35,36]. The enantioselectivity of the enzyme was expressed as the enantiomeric ratio, E , which was obtained from the equation $E = \ln[1 - c(1 + e_p)] / \ln[1 - c(1 - e_p)]$, where c is the degree of conversion and e_p the enantiomeric excess of the product [37].

RESULTS

Overexpression of EST2 in *E. coli*

We previously reported [19] on the purification of a new esterase called EST2 and its identification with the hypothetical product of the ORF3 gene. Because the EST2 protein was poorly expressed in *B. acidocaldarius*, an overexpression system in *E. coli* was devised as described in the Experimental section (Figure 1). Initial attempts were unsuccessful to subclone the gene from plasmid pKTH2000 into the PT7-7 expression vector under the control of T7 RNA polymerase Φ 10 promoter and this was most probably due to product toxicity (results not shown). This problem was overcome by the use of the expression vector PT7-SCII. The latter contains three terminator sets that should reduce the transcription starting from the ORF3 promoter included in the *Bacillus* genomic fragments that we attempted to clone. In point of fact a clone was obtained expressing EST2 at a basal level in the absence of IPTG induction. Moreover, a 2–4-fold increase of thermophilic and thermostable esterase activity was

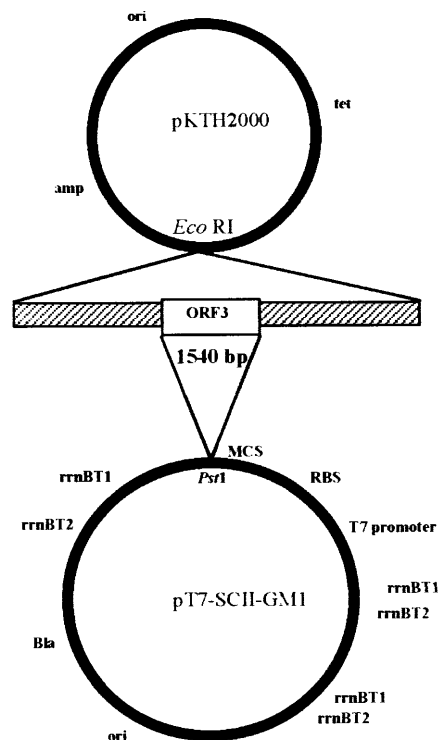


Figure 1 Construction scheme for the recombinant plasmid pT7-SCII-GM1, used for the expression of *B. acidocaldarius* EST2

The expression vector was constructed by inserting a 1540 bp *Pst*I *B. acidocaldarius* genomic fragment from plasmid pKTH2000 into the *Pst*I cloning site of plasmid pT7-SCII.

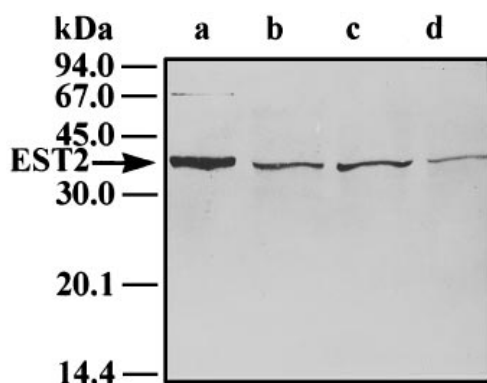


Figure 2 Western blot analysis of EST2 expression in Top 10 and BL21(DE3) *E. coli* cells

A portion (50 μ g) of total protein from Top 10 *E. coli* cells harbouring plasmid pKTH2000 (lane d), and from non-induced (lane b) or IPTG-induced (lane c) BL21(DE3) *E. coli* cells harbouring plasmid pT7-SCII-GMI, were fractionated by SDS/PAGE [12.5% (w/v) gel], transferred to a nitrocellulose sheet and treated for immunodetection as described in the Experimental section. Purified EST2 (1 μ g) (lane a) was run as control. The mobilities of molecular mass markers are indicated at the left.

Table 1 Purification scheme for recombinant EST2

Enzyme assays were performed at 70 °C with the standard assay mixture. Mean values of duplicate or triplicate measurements are reported. Standard errors of the mean were no more than 10%. Shown are the results from one purification, which is representative of three.

	Total activity (units)	Total protein (mg)	Specific activity (units/mg)	Purification (fold)
Crude extract	457300	2060	222	1.0
Thermoprecipitation at 60 °C	493000	1940	254	1.1
Thermoprecipitation at 65 °C	525000	912	576	2.6
Thermoprecipitation at 70 °C	500000	420	1190	5.4
Q Sepharose FF	451100	353	1278	5.8
Phenyl-Superose, peak (a)	167000	28.5	5860	26.4
Phenyl-Superose peak (b)	175700	69.3	2535	11.4
Mono Q FF (from peak b)	230900	54.7	4222	19.0

observed after 3 h of IPTG induction. The activity increase was fairly well correlated with the increase in proteins as judged by a Western blot analysis performed by means of a specific EST2 antiserum (Figure 2, lanes b and c). A low level of expression of EST2 was also evident in crude extracts of *E. coli* cells (Top 10) harbouring plasmid pKTH2000 (Figure 2, lane d). No reaction was observed in crude extracts of *E. coli* cells devoid of the ORF3 gene (results not shown).

EST2 purification

The purification scheme is shown in Table 1. The enzyme was purified with a 58% total yield and a purification factor of 26-fold and 19-fold in peak (a) and in peak (b) after the Mono Q column respectively (see the Experimental section). The final specific activity was approx. 5300–5900 units/mg for peak (a) and 3600–4200 units/mg for enzyme from the Mono Q Sepharose column, with the standard assay. The specific activity of peak (a) enzyme was comparable with that of the native enzyme with the same assay mixture at 37 °C [19], thus indicating that the recombinant enzyme had been correctly folded. This conclusion

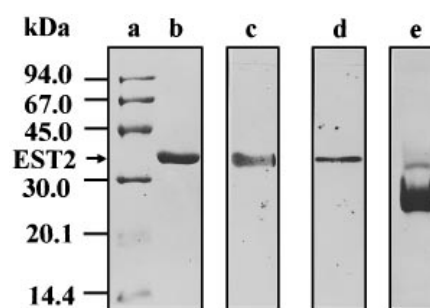


Figure 3 Electrophoretic characterization of recombinant *B. acidocaldarius* EST2

Lane a, SDS/PAGE molecular mass markers; lane b, SDS/PAGE of 5 μ g of pure recombinant EST2 from phenyl-Superose (peak a), after Coomassie staining; lane c, EST2 activity staining *in situ* after SDS/PAGE and removal of SDS; lane d, fluorography of [³H]DFP-labelled EST2 (see the Experimental section); lane e, non-denaturing 7.5% PAGE of 10 μ g of EST2 after Coomassie Blue staining.

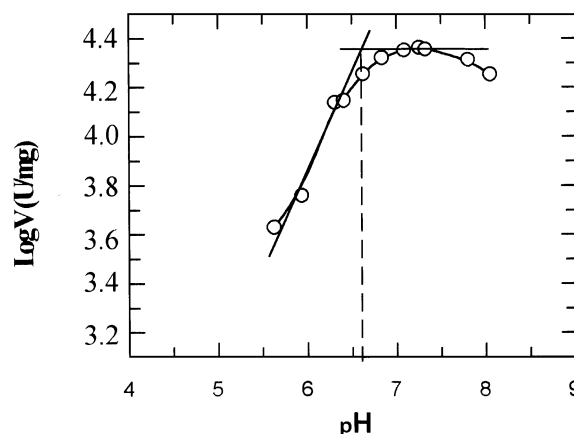


Figure 4 pH-activity profile of EST2

Activity assays of EST2 at different pH values with PNP-exanoate (0.19 mM) as substrate. The buffer used was 0.345 M Tris/HCl adjusted at 70 °C. The same result was obtained with phosphate buffer (results not shown).

was confirmed by far-UV CD measurements of the recombinant enzyme (results not shown). The proportions of structures, measured according to Yang [38], (α = 44%; β = 15%; turn = 19%; random = 22%) was in good agreement with results obtained from the secondary structure predictions (α = 35%; β = 19%; rest = 45% [19]).

Protein homogeneity was checked by reverse-phase HPLC (purity at least 98%). The enzyme was confirmed to be EST2 by means of N-terminal sequencing and molecular mass determination on SDS/PAGE. As the native enzyme [19], the recombinant protein started with a proline residue. The sequence determined was PLDPVIQQVLDQ. On SDS/PAGE [12.5% (w/v) gel] a single band of 34 kDa (Figure 3, lane b) was observed, even after staining with silver. This band was slightly active (Figure 3, lane c) after SDS removal and activity staining *in situ* and it was reactive to [³H]DFP (Figure 3, lane d). In a non-denaturing PAGE (Figure 3, lane e) mostly a single band was observed, as well as a minor slower component, which in all probability was an aggregated form. This was also observed during gel-filtration chromatography and might provide an

Table 2 Kinetic parameters for recombinant EST2 from *B. acidocaldarius*

All PNP esters were dissolved in buffer without solvents or detergent except for PNP-octanoate, which was dissolved in the standard assay mixture. Results are means \pm S.D. ($n = 3$). Each assay was done in duplicate. The enzyme concentration $[E_0]$ was 1.35 nM.

Acyl chain length	K_m (μ M)	$10^{-2}k_{cat}$ (s^{-1})	k_{cat}/K_m ($s^{-1} \cdot \mu M^{-1}$)
C ₂	124 \pm 5	6.6 \pm 0.33	5.3
C ₃	126 \pm 6	16.0 \pm 0.16	12.7
C ₄	48 \pm 5	14.2 \pm 0.99	29.5
C ₅	50 \pm 3	23.9 \pm 0.72	47.7
C ₆	11 \pm 2	66.1 \pm 8.82	600.1
C ₈	43 \pm 4	5.6 \pm 0.17	12.8

explanation for the two forms observed by phenyl-Superose chromatography.

The apparent molecular mass of the enzyme under non-

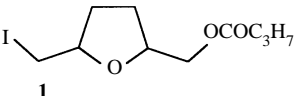
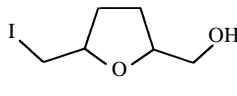
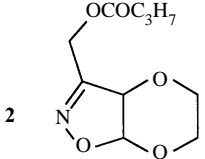
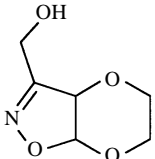
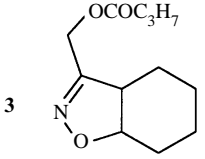
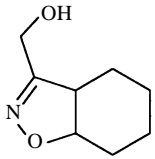
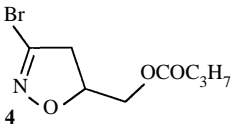
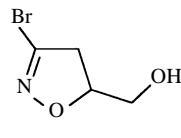
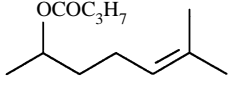
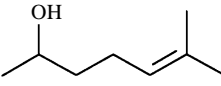
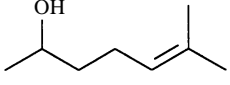
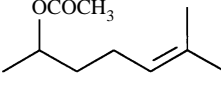
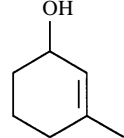
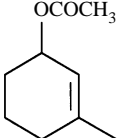
denaturing conditions was determined by gel filtration on a Zorbax GF 450 HPLC-column. A molecular mass of 34.6 kDa was estimated by interpolation on a calibration curve (results not shown). This and the above findings are consistent with a monomeric enzyme.

The optimal pH was determined at 70 °C with PNP-exanoate (C₆) as a substrate and a maximum at approx. pH 7.1 \pm 0.15 (mean \pm S.D., $n = 3$) was obtained (Figure 4). The enzyme was routinely assayed at this pH value. From the bend in the curve on the acidic side it was evident that activity depended on the ionization of a residue with an apparent pK_a of 6.7.

Kinetic studies

Table 2 displays the kinetic constants for the hydrolysis of PNP esters with acyl chain length of 2–8, at 70 °C. Substrates were dissolved in buffered solutions without solvents or detergents at concentrations 2–8-folds higher than the respective K_m values. Reaction velocity increased with increasing chain length, reaching a maximum with PNP-exanoate. Affinity constants showed a

Table 3 Enantioselectivity studies

			% c	% e.e.	E
	$\xrightarrow[\text{Buffer}]{\text{Esterase}}$		30	22	2
	$\xrightarrow[\text{Buffer}]{\text{Esterase}}$		33	38	3
	$\xrightarrow[\text{Buffer}]{\text{Esterase}}$		44	35	3
	$\xrightarrow[\text{Buffer}]{\text{Esterase}}$		36	84	18
	$\xrightarrow[\text{Buffer}]{\text{Esterase}}$		28	60	5
	$\xrightarrow[\text{Toluene}]{\text{Esterase, Vinyl acetate}}$		34	38	3
	$\xrightarrow[\text{Toluene}]{\text{Esterase, Vinyl acetate}}$		27	61	5

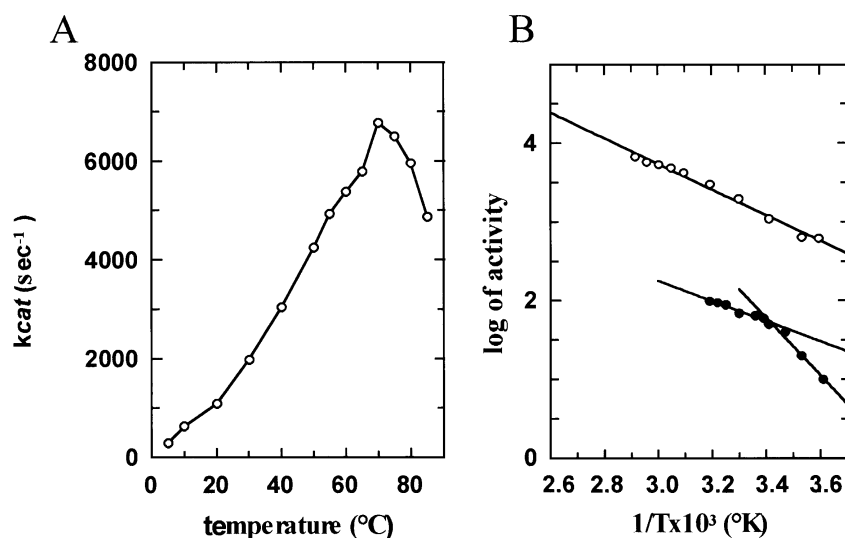


Figure 5 Temperature dependence of EST2

(A) EST2 activity was measured at different temperatures with the standard assay. (B) Values from (A) were plotted (○) on an Arrhenius plot. Also shown are results for MOL (●) replotted from [6]. Correlation coefficients were -0.993 for EST2 and -0.983 and -0.986 for MOL (high and low temperature range respectively).

decrease as chain length increased. For the best substrate (C_6) a k_{cat} of $6610 \pm 800 \text{ s}^{-1}$ (mean \pm S.D., $n = 3$) and a K_m of $11 \pm 2 \mu\text{M}$ (mean \pm S.D., $n = 3$) were estimated. The activity towards longer PNP esters (C_{12} and C_{16}), dissolved in detergents and organic solvents, proved detectable, albeit very low (results not shown).

Because EST2 shows sequence identity with the lipases of the HSL subgroup and with CRL [1,19], the lipase activity of this enzyme was tested with [¹⁴C]trioleoylglycerol. No activity was detected under the conditions used.

A relatively high identity (33%) of EST2 was previously found [19] with a recently identified HDAC [10]. For this reason EST2 was tested for amidase activity. No activity was detected with PNP-acetamide as a substrate.

Enantioselectivity studies

The results obtained in the esterase-catalysed resolution of several racemic alcohols of interest in the pharmaceutical or pheromone field [33–36] are summarized in Table 3. The enzyme was very effective as a catalyst; significant conversions were achieved in short reaction periods and with high substrate-to-enzyme ratios. However, substantial enantioselectivity was observed only in the resolution of compound **4**, where the (*R*)-product was obtained with an 84% enantiomeric excess at 36% conversion. The enantiomeric ratios were between 2 and 18. The enzyme was also able to synthesize acetyl esters (from compounds **6** and **7** in Table 3) when tested in vinyl acetate and toluene. In contrast with what was observed with other enzymes, the use of an organic solvent as the reaction medium did not improve enzyme selectivity (compare **5** and **6** in Table 3).

Thermophilicity and thermostability

The relationship between activity and temperature over the range 5–85 °C was obtained with PNP-exanoate as a substrate (Figure 5A). The optimal temperature was found to be 70 °C. An energy activation value of 31 kJ/mol (7.4 kcal/mol) was esti-

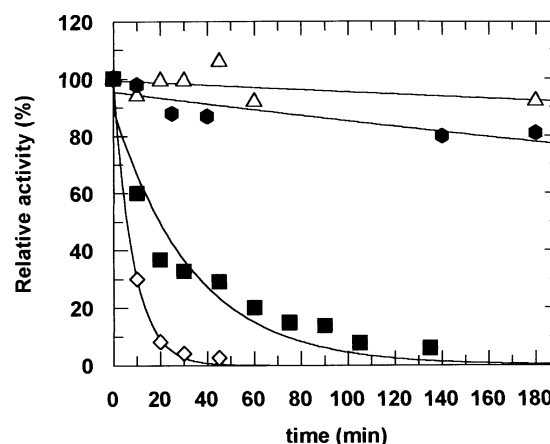


Figure 6 Thermostability of EST2

The enzyme was incubated in sealed glass vials, in 10 mM Tris/HCl at 70 °C (△), 75 °C (●), 80 °C (■) and 90 °C (◇). Samples were withdrawn at the indicated times and assayed by the standard assay. Data are reported as a percentage of the activity of a non-incubated sample. Data points were computer-fitted to curves in accordance with a theoretical rate equation for single-exponential decay.

mated from the linear part of the Arrhenius plot over the range 5–70 °C (Figure 5B).

The thermal stability of the esterase (125 μg/ml) was studied by measuring the residual activity after incubation for different periods at temperatures ranging between 70 and 90 °C (Figure 6). In the conditions outlined the enzyme was stable at 70 °C for more than 14 h and stable at 75 °C for at least 3 h. At 80 and 90 °C the enzyme had a $t_{1/2}$ of approx. 30 and 10 min respectively. Enzyme stability decreased with decreasing protein concentration (results not shown).

Table 4 shows a comparison of the amino acid compositions of MOL, ACE, HSL and EST2. The Cys content and the Asn

Table 4 Comparison of amino acid compositions

Amino acid compositions were all obtained from the respective published sequences. For HSL the results do not change significantly if the phosphorylation domain [1] is excluded from the computation. Trends of amino acid changes are in bold type-face.

Amino acids	MOL		ACE		HSL		HSL		EST2	
	No.	Mole%	No.	Mole%	No.	Mole%	No.	Mole%	No.	Mole%
Ala	50	11.55	28	8.70	80	10.32	68	10.63	37	11.94
Cys	8	1.85	4	1.24	14	1.81	14	2.19	1	0.32
Asp	26	6.00	21	6.52	31	4.00	25	3.91	21	6.77
Glu	19	4.39	16	4.97	48	6.19	35	5.47	20	6.45
Phe	9	2.08	15	4.66	33	4.26	29	4.53	12	3.87
Gly	26	6.00	16	4.97	58	7.48	48	7.50	22	7.10
His	17	3.93	10	3.11	18	2.32	17	2.66	8	2.58
Ile	19	4.39	19	5.90	22	2.84	21	3.28	11	3.55
Lys	21	4.85	16	4.97	16	2.06	12	1.88	12	3.87
Leu	52	12.01	45	13.98	107	13.81	90	14.06	34	10.97
Met	6	1.39	7	2.17	19	2.45	15	2.34	6	1.94
Asn	21	4.85	10	3.11	19	2.45	14	2.19	6	1.94
Pro	25	5.77	23	7.14	55	7.10	43	6.72	28	9.03
Gln	25	5.77	19	5.90	24	3.10	20	3.12	12	3.87
Arg	13	3.00	13	4.04	56	7.23	46	7.19	16	5.16
Ser	26	6.00	17	5.28	72	9.29	51	7.97	13	4.19
Thr	25	5.77	17	5.28	41	5.29	34	5.31	8	2.58
Val	25	5.77	13	4.04	40	5.16	37	5.78	23	7.42
Trp	6	1.39	3	0.93	6	0.77	5	0.78	4	1.29
Tyr	14	3.23	10	3.11	16	2.06	16	2.50	16	5.16

Table 5 Effect of inhibitors on recombinant EST2

The enzyme (67.5 µg/ml) was incubated at 37 °C in 50 mM Tris/HCl, pH 8, for 5 min, with different concentrations of the inhibitor. Results are the means for two experiments. Each assay was done in duplicate or triplicate with the standard assay.

Inhibitor	Concentration (M)	Residual activity (%)
PMSF	0.10×10^{-3}	0.0
	0.01×10^{-3}	24.4
Physostigmine	0.05×10^{-3}	2.0
	0.03×10^{-3}	6.0
	0.01×10^{-3}	14.0
Diethyl- <i>p</i> -nitrophenylphosphate	0.50×10^{-6}	0.0
	0.10×10^{-6}	33.8
	0.05×10^{-6}	61.5
Diethyl pyrocarbonate	5.0×10^{-3}	1.9
	2.0×10^{-3}	5.6
	1.0×10^{-3}	17.3
	0.5×10^{-3}	28.0
	0.1×10^{-3}	61.7

content decreased moving from the psychrophilic to the thermophilic enzyme, whereas the Pro and Glu contents increased.

Inhibitors

Table 5 shows the effect of several inhibitors. The enzyme was rapidly inhibited by the organophosphate diethyl-*p*-nitrophenylphosphate at very low concentrations (50 nM), whereas physostigmine, a carbamate-type inhibitor, was effective at a 1000-fold higher concentration. PMSF inhibited the enzyme to the same degree, at a concentration of 100 µM. The inhibition was essentially irreversible as judged by the activity assay of the enzyme after exhaustive dialysis or gel filtration, and by the

stability of the [³H]DFP-labelled enzyme to SDS/PAGE conditions (Figure 3, lane c). Diethyl pyrocarbonate at a low concentration (5 mM) almost completely inhibited the enzyme, suggesting the involvement of a histidine residue at the active site.

Active-site titration

To determine the number of active sites per molecule of the enzyme, a known amount of pure protein was titrated with [³H]DFP, as described in the Experimental section. Assuming a molecular mass of 34 kDa, 1.4 ± 0.2 mol (mean \pm S.D., $n = 3$) of [³H]DFP were required to titrate 1 mol of the enzyme. When the enzyme was preincubated with diethyl pyrocarbonate before labelling with [³H]DFP, a marked decrease in bound radioactivity was observed (results not shown). This finding suggests that the two inhibitors bind at the same enzymic site.

Cysteine titration

By sequence inspection we noticed that a single cysteine residue (Cys-101) occurs in the enzyme. We wondered whether or not this residue was involved in the enzyme's active site, as reported for *Bacillus stearothermophilus* NCA2184 carboxylesterase [14] and whether or not it was fully exposed to the solvent. Ellmann's reagent, as described in the Experimental section, was used to titrate the thiol group under native conditions. The reaction proceeded very quickly and was complete in less than 1 min. A single exposed cysteine residue was estimated on the basis of a protein molecular mass of 34 kDa and a molar absorption coefficient of $13600 \text{ M}^{-1} \cdot \text{cm}^{-1}$ at 412 nm for the 2-nitro-5-thiobenzoate anion. The activity of the modified enzyme in the standard assay was found to be the same as that of the control.

DISCUSSION

An efficient overexpression system of the ORF3 gene was devised in *E. coli* and biochemical studies were performed on the recombinant thermostable enzyme.

As described in the Results section, although high-level expression was attained under the control of the ORF3 promoter and ribosome-binding site, a further 2–4-fold expression increase was nevertheless obtained after 3 h of IPTG induction. This can be ascribed to the generalized increase in transcription starting from the $\Phi 10$ promoter of pT7-SCII plasmid after IPTG induction.

As inferred from SDS/PAGE, gel-permeation chromatography and titration of the active site with [³H]DFP, the enzyme was a 34 kDa monomer with a single active centre, similar to the EST1 previously purified from *B. acidocaldarius* [17].

Occasionally EST2 showed inhibition by excess of substrate. This effect was observed above a certain concentration, which was different for each ester and was dependent on the respective acyl chain length as well as on the age of the ester stock solutions (results not shown). When detergents and solvents were present in the assay mixtures, inhibition disappeared. In the light of the above, this phenomenon could be ascribed to the formation of micelles. A similar phenomenon was described for *B. stearothermophilus* NCA2184 carboxylesterase [14].

As regards substrate specificity, the profile shown in Table 2 suggests the presence at the active site of a hydrophobic binding pocket able to accommodate short and medium-length acyl chains. This profile is rather different from that obtained for *B. acidocaldarius* EST1 [17] and very similar to that obtained for *B. stearothermophilus* NCA2184 carboxylesterase [14]. The latter

enzyme is similar to EST2 in a number of other features such as optimal pH, thermophilicity and DFP sensitivity but different in its apparent molecular mass, thermostability and sensitivity to thiol reagents. A systematic study on enzyme specificity for esters with different alcoholic moieties is required before any assumption can be made about the physiological role of these enzymes. Unfortunately, this is still an open question for a number of systems. A physiological role in drug detoxification pathways has only recently been demonstrated for a few enzymes [39,40].

The inhibitory effect of diethyl-*p*-nitrophenylphosphate, physostigmine, PMSF and diethyl pyrocarbonate (Table 5), as well as the competition between the latter and [³H]DFP labelling, suggested the involvement of a serine residue and a histidine residue at the active site. This was in agreement with the previous prediction of a 'catalytic triad' composed of Ser-155, His-282 and Asp-252 [19], as well as with the pH activity profile shown in Figure 4, which indicates that a residue with a pK_a of 6.7, probably histidine, is present at the active site. Experiments to mutagenize these residues are currently in progress.

On the basis of both the substrate specificity (Table 2) and the sensitivity to carbamate and organophosphate-type inhibitors (Table 5), EST2 should be classified, in accordance with Oosterbaan and Jansz [41], as a B'-type carboxylesterase (EC 3.1.1.1).

The enzyme showed remarkable temperature stability as it was stable at 70 °C for at least 14 h and had a $t_{1/2}$ of 3 h at 75 °C (Figure 6). This property is of valuable biotechnological interest. Although EST2 was more stable than both *B. acidocaldarius* EST1 [17] and the carboxylesterase from *B. stearothermophilus* NCA2184 [14], it was less stable than an esterase from *S. acidocaldarius* [13] but equally thermostable as the esterase purified from *B. stearothermophilus* Tok19A1 [16].

The HSL subfamily includes hydrolases from bacteria and eukaryotes, as well as from psychrophilic, mesophilic and thermophilic sources [1]. Comparative studies within this group would be of valuable interest in the field of protein stability determinants. In the current absence of any three-dimensional structure for members of the HSL group, an attempt was made to analyse the amino acid compositions (Table 4) of EST2, HSL, MOL and ACE, four enzymes of the HSL group that act on similar substrates (i.e. acyl esters). This analysis quite unexpectedly revealed some trends in amino acid changes that are presumably related to both protein thermal stability and/or thermophilicity. A clear decrease was observed in the Cys and Asn content, as expected for residues that are sensitive to oxidation and deamidation respectively at high temperature [42], whereas proline residues, commonly responsible for higher protein rigidity and therefore thermal stability [43,44] increased. The increase in the Glu content was somewhat more complicated to interpret as there was no parallel increase in Lys and/or Arg residues, which might be the counterions in salt bridges believed to have a pivotal role as determinants of protein stability ([45,46], and references therein).

Mammalian HSL displays unusual properties. In particular it shows high activity at low temperatures; this was attributed to the (relatively) high identity with MOL [3]. The finding that a thermophilic esterase shares homology with both the psychrophilic MOL and mesophilic mammalian enzymes (HSL and HDAC) suggests that caution should be made when correlating sequence identity with thermal behaviour.

The EST2 activity-temperature relationship was investigated by using Arrhenius plots. EST2 displayed optimal activity at 70 °C, corresponding to the *B. acidocaldarius* optimal growth temperature (Figure 5A). The Arrhenius plot (Figure 5B) was

linear over the range 5–70 °C; thus no change in activation energy was observed. Beyond 85 °C enzyme denaturation was likely to occur as suggested by activity measurements (Figures 5A and 6) and changes in the spectroscopic behaviour of the enzyme (results not shown). At 5 °C EST2 was still detectable, with approx. 5% of the activity at 70 °C. This feature, besides being of valuable biotechnological interest, suggested the possibility to make comparisons between thermophilic, mesophilic and psychrophilic enzymes in the same temperature range, as well as at their respective optimal temperatures. For this purpose published data of activity against temperature for MOL [6] obtained with PNP-butyrate as a substrate, were replotted in Figure 5(B) and a breakpoint was observed at approx. 20 °C. Although the two enzymes have different optimal temperatures (70 and 40 °C respectively), the calculated activation energies in the range 40–20 °C are roughly comparable with a slight increase going from MOL [E_a 24.1 kJ/mol (5.75 kcal/mol)] to EST2 [E_a 31.1 kJ/mol (7.44 kcal/mol)]. This means comparable catalytic activities for the two enzymes when considering activity towards similar substrates. The downward curvature at low temperature observed for several thermophilic enzymes ([47], and references therein) and generally interpreted as being due to lower conformational flexibility [47,48] was not detected for EST2 and was instead observed for MOL in the range 20–5 °C, where the activation energy was twice that of EST2. This might suggest an unusual higher flexibility at low temperatures in this thermostable enzyme, thus agreeing with data reported for HSL [3]. Unfortunately the latter were insufficient for an analysis in terms of activation energy and slope changes in the Arrhenius plot.

In conclusion it seems that among enzymes analysed so far, it is not only mammalian HSL in the HSL subfamily that presents an unusual activity-temperature relationship. Owing to the thermal stability of EST2, the observed similarity in thermal behaviour at low temperature between HSL and EST2 can be ascribed to a greater flexibility in the active site, the occurrence of which can be demonstrated only by comparing the respective three-dimensional structures.

Previous analyses of the EST2 sequence [19] made it possible to identify the *Candida rugosa* lipase [49] as remotely homologous (26% identity in a global alignment). EST2 did not show lipase activity, and this indicated differences at the substrate-binding-site level. This suggestion is in line with previous conclusions that the α/β -hydrolase fold represents a useful and quite flexible scaffold utilized by evolution to build new hydrolytic enzymes [50]. It is worth mentioning that the region of EST2 corresponding to the 'lid' in *C. rugosa* lipase [51] seems to be partly deleted in a multisequence alignment [19]. This finding, together with the inhibition caused by substrate excess (true lipases are activated) and the absence of activity with trioleoylglycerol, supports the conclusion that the enzyme is not a lipase.

A larger set of substrates requires investigation to establish the synthetic utility of the enzyme. Furthermore protein engineering and medium engineering must also be explored systematically to improve enantioselectivity.

We thank Professor I. Palva for supplying plasmid pKTH2000, Dr. S. D'Auria for far-UV CD measurements, V. Carratore for performing the N-terminal sequencing, R. Defez for help in the antiserum preparation, and G. Imparato and O. Piedimonte for technical assistance. This study was partly supported by a European Union Contract (B104-CT96-0488) and by an INTAS project (94-4105)

REFERENCES

- 1 Hemilä, H., Koivula, T. T. and Palva, I. (1994) *Biochim. Biophys. Acta* **1210**, 249–253

- 2 Krejci, E., Duval, N., Chatonnet, A., Vincens, P. and Massoulié, J. (1991) *Proc. Natl. Acad. Sci. U.S.A.* **88**, 6647–6651
- 3 Langin, D., Laurell, H., Stenson Holst, L., Belfrage, P. and Holm, C. (1993) *Proc. Natl. Acad. Sci. U.S.A.* **90**, 4897–4901
- 4 Raibaud, A., Zalacain, M., Holt, T., Tizard, R. and Thompson, C. J. (1991) *J. Bacteriol.* **173**, 4454–4463
- 5 Wohleleben, W., Arnold, W., Broer, I., Hillemann, D., Strauch, E. and Puhler, A. (1988) *Gene* **70**, 25–37
- 6 Feller, G., Thiry, M., Arpigny, J. L. and Gerday, C. (1991) *Gene* **102**, 111–115
- 7 Alon, R. N. and Gutnick, D. L. (1993) *FEMS Microbiol. Lett.* **112**, 275–280
- 8 Peist, R., Koch, A., Bolek, P., Sewitz, S., Kolbus, T. and Boos, W. (1997) *J. Bacteriol.* **179**, 7679–7686
- 9 Singleton, C. K., Manning, S. S. and Ken, R. (1989) Submitted to EMBL/GenBank/DBJ data banks, Swiss-Prot accession number p14326
- 10 Probst, M. R., Beer, M., Beer, D., Jenö, P., Meyer, V. A. and Gasser, R. (1994) *J. Biol. Chem.* **269**, 21650–21656
- 11 Sarda, L. and Desnuelle, P. (1958) *Biochim. Biophys. Acta* **159**, 285–295
- 12 Martínez, C., de Geus, P., Lauwereys, M., Matthysens, G. and Cambillau, C. (1992) *Nature (London)* **356**, 615–618
- 13 Sobek, H. and Gorish, H. (1989) *Biochem. J.* **250**, 453–458
- 14 Matsunaga, A., Koyama, N. and Nosoh, Y. (1974) *Arch. Biochem. Biophys.* **160**, 504–513
- 15 Owusu, R. K. and Cowan, D. A. (1991) *Enzyme Microb. Technol.* **13**, 158–163
- 16 Wood, A. N., Fernandez-Lafuente, R. and Cowan, D. A. (1995) *Enzyme Microb. Technol.* **17**, 816–825
- 17 Manco, G., Di Gennaro, S., De Rosa, M. and Rossi, M. (1994) *Eur. J. Biochem.* **221**, 965–972
- 18 Schmidt-Dannert, C., Rua, M. L., Atomi, H. and Schmid, R. D. (1996) *Biochim. Biophys. Acta* **1301**, 105–114
- 19 Manco, G., Adinolfi, E., Pisani, F. M., Carratore, V. and Rossi, M. (1997) *Protein Peptide Lett.* **4**, 375–382
- 20 Koivula, T. T., Hemilä, H., Pakkanene, R., Sibakov, M. and Palva, I. (1993) *J. Gen. Microbiol.* **139**, 2399–2407
- 21 Studier, F. W. and Moffatt, B. A. (1986) *J. Mol. Biol.* **189**, 113–130
- 22 Brown, W. C. and Campbell, J. L. (1993) *Gene* **127**, 99–103
- 23 Sambrook, J., Fritsch, E. F. and Maniatis, T. (1989) *Molecular Cloning: A Laboratory Manual*, 2nd edn., Cold Spring Harbor Laboratory, Cold Spring Harbor, NY
- 24 Dixon, M. and Webb, E. C. (1979) in *Enzymes*, 3rd edn., Longman, London
- 25 Leatherbarrow, R. J. (1992) *GraFit Version 3.0*, Erithacus Software Ltd., Staines, U.K.
- 26 Heymann, E. and Mentlein, R. (1981) *Methods Enzymol.* **77**, 533–544
- 27 Enholm, C. and Kuusi, T. (1986) *Methods Enzymol.* **129**, 717–738
- 28 Laemmli, U. K. (1970) *Nature (London)* **227**, 680–685
- 29 Higerd, T. B. and Spizizen, J. (1973) *J. Bacteriol.* **114**, 1184–1192
- 30 Waterborg, J. H. and Matthews, H. R. (1984) in *Methods in Molecular Biology* (Walker, J. M., ed.), vol. 1, pp. 147–152, Humana Press, New Jersey
- 31 Habeeb, A. F. S. A. (1972) *Methods Enzymol.* **25**, 457–464
- 32 Matsudaira, P. (1987) *J. Biol. Chem.* **262**, 10035–10038
- 33 Ottolina, G., Bovara, R., Riva, S. and Carrea, G. (1994) *Biotechnol. Lett.* **16**, 923–928
- 34 Orrenius, C., Norin, T., Hult, K. and Carrea, G. (1995) *Tetrahedron: Asymmetry* **6**, 3023–3030
- 35 De Amici, M., De Micheli, C., Carrea, G. and Riva, S. (1996) *Tetrahedron: Asymmetry* **7**, 787–796
- 36 De Amici, M., Magri, P., De Micheli, C., Cateni, F., Bovara, R., Carrea, G., Riva, S. and Casalone, G. (1992) *J. Org. Chem.* **57**, 2825–2829
- 37 Chen, C.-S., Fujimoto, Y., Girdaukas, G. and Sih, C. J. (1982) *J. Am. Chem. Soc.* **104**, 7294–7299
- 38 Yang, J. T. (1986) *Methods Enzymol.* **130**, 208–269
- 39 Varki, A., Muchmore, E. and Diaz, S. (1986) *Proc. Natl. Acad. Sci. U.S.A.* **83**, 882–886
- 40 Reddy, T. V., Weissburger, E. K. and Thorgeirsson, S. S. (1980) *J. Natl. Cancer Inst.* **64**, 1563–1569
- 41 Oosterbaan, R. A. and Jansz, H. S. (1965) in *Comprehensive Biochemistry*, vol. 16, (Florkin, M. and Stoltz, E. H., eds.), pp. 1–54, Elsevier, Amsterdam
- 42 Zale, S. E. and Klibanov, A. M. (1986) *Biochemistry* **25**, 5432–5444
- 43 Matthews, B. W. (1993) *Annu. Rev. Biochem.* **62**, 139–160
- 44 Watanabe, K., Chishiro, K., Kitamura, K. and Suzuki, Y. (1991) *J. Biol. Chem.* **266**, 24287–24294
- 45 Vieille, C. and Zeikus, J. G. (1996) *Trends Biotechnol.* **14**, 183–190
- 46 Aguilar, C. F., Sanderson, I., Moracci, M., Ciaramella, M., Nucci, R., Rossi, M. and Pearl, L. H. (1997) *J. Mol. Biol.* **271**, 789–802
- 47 Wrba, A., Schweiger, A., Schultes, V. and Jaenicke, R. (1990) *Biochemistry* **29**, 7584–7592
- 48 Vihinen, M. (1987) *Protein Eng.* **1**, 477–480
- 49 Kawaguchi, Y., Honda, H., Taniguchi-Morimura, J. and Iwasaki, S. (1989) *Nature (London)* **341**, 164–166
- 50 Ollis, D. L., Cheah, E., Cygler, M., Dijkstra, B., Frolow, F., Franken, S. M., Harel, M., Remington, S. J., Silman, I., Schrag, J. D. et al. (1992) *Protein Eng.* **5**, 197–211
- 51 Grochulski, P., Li, Y., Schrag, J. D., Bouthillier, F., Smith, P., Harrison, D., Rubin, B. and Cygler, M. (1993) *J. Biol. Chem.* **268**, 12843–12847